*Journal of Applied Mechanics and Technical Physics, Vol. 46, No. 3, pp. 444–451, 2005*

# STRESS ANALYSIS OF CONCRETE AND REINFORCED-CONCRETE SLAB STRUCTURES UNDER A HIGH-VELOCITY IMPACT

**N. N. Belov, N. T. Yugov, D. G. Kopanitsa, and A. A. Yugov**

UDC 539.3

*A mathematical model is developed, which describes the behavior of reinforced concrete under high-velocity impact and explosion conditions within the framework of mechanics of continuous media. The problem of a model projectile penetrating into a layered target consisting of two concrete slabs separated by a sand layer and blasting of an explosive charge encased in the embedded projectile is solved in the three-dimensional formulation by the finite-element method. The effect of reinforcement on penetration and failure of reinforced-concrete slabs is studied by means of mathematical simulations.*

**Key words:** *impact, failure, concrete, reinforced concrete, mathematical simulation.*

In designing protective structures of underground installations, it is necessary to estimate their resistance to high-rate dynamic loads. This problem can effectively be solved by mathematical simulation of deformation and failure of these structures subjected to an impact or explosion.

The problem of the impact interaction between cylindrical metal impactors and concrete targets was solved in [1, 2]. To study concrete failure, a phenomenological approach was applied, where the strength criteria are expressed in terms of invariant relations between the critical values of macrocharacteristics of the process: stresses and strains. A comparison of mathematical simulations with the results of a special experiment showed that this approach to the failure problem, used to solve static problems, can also be used to analyze concrete failure under dynamic loads.

A mathematical model was developed in [3, 4] to analyze the behavior of sandy soil under shock-wave loading. The processes of penetration of cylindrical and star-shaped impactors into a sandy half-space were studied by the method of computer modeling. The effect of the impactor shape on the penetration depth was revealed [4]. The problem of cylindrical impactors penetrating into structures composed of sandy soil and concrete was solved in a three-dimensional formulation [3].

Much attention has been given to mathematical simulation of collisions of solid bodies with various monolithic and layered targets made of metal, ceramics, and composite materials (see, e.g., [5–8]). However, calculating the penetration of solids into reinforced-concrete slabs is still an open question. Results of experimental and theoretical studies on the impact interaction of cylindrical bodies with ogival head parts with concrete and reinforced-concrete slabs within the impact-velocity range of 100–650 m/sec and the impact-angle range of 0–40° (the angle is counted from the normal to the target surface) can be found in [9]. In the experiments performed, the impactor diameter was smaller than the characteristic size of the reinforcing grid cell. The experimental studies show that reinforcement of a concrete target improves its bearing capacity by preventing the global failure but has little influence on the character of local failure. It follows from the experimental and theoretical results that concrete reinforcement affects the penetration of solids into typical reinforced-concrete targets only slightly. The present paper considers a

Tomsk State University of Architecture and Civil Engineering, Tomsk 634003; serna@snark.ipme.ru. Translated from Prikladnaya Mekhanika i Tekhnicheskaya Fizika, Vol. 46, No. 3, pp. 165–173, May–June, 2005. Original article submitted May 12, 2004; revision submitted July 20, 2004.

 

calculation method for predicting the strength of a structure composed of concrete, reinforced-concrete, and sandy-soil layers upon penetration and initiation of impactors containing explosive charges at various penetration depths. The impactor diameter can exceed the characteristic size of the reinforcing grid cell.

**1. Mathematical Model.** A mathematical model that allows one to describe the behavior of deformable solids under high-velocity impact and explosion conditions is proposed in [6]. The cleavage failure of ductile materials is considered as the process of growth and coalescence of voids in a plastically deformed material under tensile stresses. In this approach, the limiting value of the relative volume of voids is used as the local strength criterion of a material. The limiting value of the plastic-deformation work is used as the local criterion of shear rupture.

To solve the problem of the impact interaction of a metal impactor of an arbitrary shape with reinforced-concrete slabs, we use the model of a porous elastoplastic body [6].

We represent the volume of the porous medium $v$ as the sum of the specific volume of the matrix $v_m$ and the specific volume of pores $v_p$. The material porosity is characterized by the relative volume of pores $\xi$ or by the parameter $\alpha = v/v_m$ related by $\alpha = 1/(1-\xi)$.

The motion of a porous elastoplastic medium is described by the following system of equations, which comprises the laws of conservation of mass, momentum, and energy:

$$\frac{d}{dt}\int\limits_V \rho\, dV = 0, \qquad \frac{d}{dt}\int\limits_V \rho\boldsymbol{u}\, dV = \int\limits_s \boldsymbol{n}\cdot\sigma\, dS, \qquad \frac{d}{dt}\int\limits_V \rho E\, dV = \int\limits_s \boldsymbol{n}\cdot\sigma\cdot\boldsymbol{n}\, dS;$$

$$e = s^j/(2\mu) + \lambda s, \qquad s : s = (2/3)\sigma_T^2; \tag{1.1}$$

$$p = \frac{\rho_{m0}}{\alpha}\Big[\frac{c_{m0}^2(1-\gamma_{m0}\eta/2)}{(1-q_{m0}\eta)^2}\,\eta + \gamma_{m0}\varepsilon\Big]. \tag{1.2}$$

Here $t$ is the time, $V$ is the domain of integration, $S$ is the surface area of the latter, $\rho$ is the material density, $\boldsymbol{n}$ is the vector normal to the surface, $\sigma = -pg + s$ is the stress tensor, $s$ is the stress-tensor deviator, $p$ is the pressure, $g$ is the metric tensor, $\boldsymbol{u}$ is the velocity vector, $E = \varepsilon + \boldsymbol{u}\cdot\boldsymbol{u}/2$ is the total specific energy, $\varepsilon$ is the specific internal energy, $e = d - (d : g)g/3$ is the deviator of the strain-rate tensor, $d = (\nabla\boldsymbol{u} + \nabla\boldsymbol{u}^{\mathrm{t}})/2$ is the strain-rate tensor, $s^j = \dot{s} + s\cdot\omega - \omega\cdot s$ is the derivative of the stress deviator in the Jaumann–Noll sense, $\mu = \mu_{m0}(1-\xi)[1-\xi(6\rho_{m0}c_{m0}^2 + 12\mu_{m0})/(9\rho_{m0}c_{m0}^2 + 8\mu_{m0})]$ and $\sigma_T$ are the effective shear modulus and yield stress, respectively, $\omega = (\nabla\boldsymbol{u}^{\mathrm{t}} - \nabla\boldsymbol{u})/2$ is the vortex tensor, $q_{m0}$, $\rho_{m0}$, and $c_{m0}$ are the material constants, $\eta = 1 - \rho_{m0}v/\alpha$, and $\gamma_{m0}$ is the Grüneisen coefficient of the matrix material. The parameter $\lambda$ is eliminated using the yield criterion.

To close system (1.1), (1.2), the equation governing the variation of the parameter $\alpha$ under extension is taken in the form [6]

$$\frac{d\alpha}{dt} = -\frac{(\alpha_0-1)^{2/3}}{\eta_1}\,(\alpha-1)^{1/3}\Delta p. \tag{1.3}$$

It is used for $\Delta p = p + (a_s/\alpha)\ln(\alpha/(\alpha-1)) < 0$.

Compaction and collapse of pores under compression after preliminary loosening is described by Eq. (1.3) provided that

$$\Delta p = p - \frac{2\sigma_s}{3\alpha}\,\ln\frac{\alpha}{\alpha-1} > 0.$$

Otherwise, $d\alpha/dt = 0$. The following notation is introduced: $\alpha_0$ is the initial porosity of the material and $\eta_1$ and $a_s$ are the material constants.

For metals, we obtain $\sigma_T = \sigma_s/\alpha$, where $\sigma_s$ is the yield stress of the matrix material. For $\alpha = \alpha_0 = 1.0003$ and $\lambda = 0$, system (1.1)–(1.3) describes deformation of the matrix material according to the model of an elastic solid.

Concrete under dynamic loading up to its failure is described by the model of a linearly elastic solid with physicomechanical properties of concrete. After failure, this becomes an isotropically hardened elastoplastic solid with physicomechanical properties of a granular medium. The shear-strain resistance of this medium is much lower

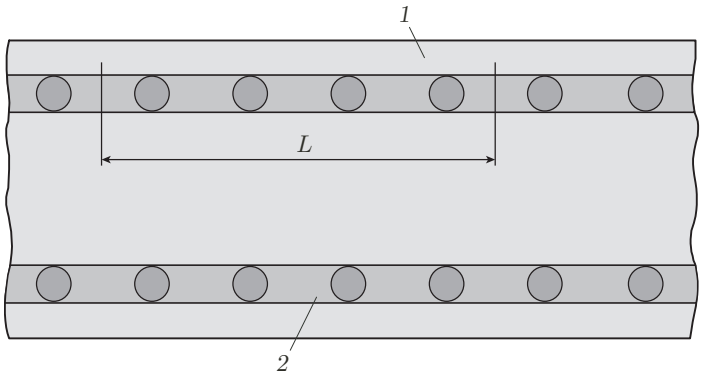


Fig. 1. Schematic diagram of reinforced concrete: 1) concrete; 2) concrete layer with a reinforcing grid.

than that of concrete before failure, and this medium cannot withstand tensile stresses. For failed concrete, the yield stress depends on pressure and is given by the formula

$$\sigma_T = \sigma_{\min} + \frac{(\sigma_{\max} - \sigma_{\min})k_1 p}{(\sigma_{\max} - \sigma_{\min}) + k_1 p},$$

where $k_1 = 0.82$, $\sigma_{\min} = 0.0077$ GPa, and $\sigma_{\max} = 0.0216$ GPa.

We use the strength criterion proposed for concrete in [10], namely,

$$3I_2 = [AI_1 + B]\{1 - (1 - C)[1 - (I_3/2)(I_2/3)^{-3/2}]\}, \tag{1.4}$$

where $I_1$ and $I_2$ and $I_3$ are the first invariant of the stress tensor and the second and third invariants of the stress deviator, respectively, $A = R_c - R_p$, $B = R_c R_p$, and $C = 3T_c^2/(R_c R_p)$, where $R_c$, $R_p$, and $T_c$ are the ultimate strengths under uniaxial compression, tension, and pure shear.

The numerical values of $A$, $B$, and $C$ are determined in terms of the compressive, tensile, and shear strengths of concrete, respectively, obtained under dynamic loading [10]. Figure 1 shows a schematic diagram of a reinforced-concrete slab. In calculating reinforced-concrete slabs, the layer of concrete with reinforcement is modeled by an elastoplastic medium that is a homogeneous two-phase mixture of steel and concrete with the initial density $\rho_{s0}$ determined as

$$\rho_{s0} = \nu_1 \rho_{10} + \nu_2 \rho_{20},$$

where $\nu_1$, $\nu_2$, $\rho_{10}$, and $\rho_{20}$ are the initial volume concentrations and densities of steel and concrete ($\nu_1 + \nu_2 = 1$).

The volume concentrations are expressed via the areas occupied by steel and concrete in the cross section normal to the reinforcing bar

$$\nu_1 = \pi d_1 n/(4L), \qquad \nu_2 = 1 - \nu_1,$$

where $L$ is the length, $n$ is the number of bars within a segment of length $L$, and $d_1$ is the bar diameter.

The equation of state of reinforced concrete (mixture) has the form

$$p = \rho_{s0} c_0^2 \eta (1 - \gamma_s \eta/2)/(1 - q\eta)^2 + \gamma_s \rho_{s0} \varepsilon, \qquad \eta = 1 - \rho_{s0} v/\alpha,$$

where $v$ is the specific volume of the mixture, $\gamma_s$ is the Grüneisen coefficient, and $v_{s0} = 1/\rho_{s0}$.

The coefficients $c_0$ and $q$ in the linear equation $D = c_0 + qu$ that relates the shock-wave velocity $D$ in the mixture to the mass velocity $u$ are determined via the shock adiabats of the mixture components:

$$D_i = c_{i0} + q_i u_i \qquad (i = 1, 2).$$

In the variables $(v, p)$, the shock adiabat of the mixture has the form

$$v(p) = \sum_{i=1}^{2} m_i \Big\{ v_{i0} - \frac{1}{p} \Big[ \frac{c_{i0}}{q_i} \sqrt{\frac{p}{\rho_{i0} c_{i0}^2} + \frac{1}{4}} - \frac{1}{2} \Big]^2 \Big\},$$

TABLE 1

| $\rho_{m0}$, g/cm$^3$ | $c_{m0}$, cm/$\mu$sec | $q_{m0}$ | $\gamma_0$ | $\gamma_H$ | $n$ | $A\rho_H^{n-1}/D_H^2$ |
|---|---|---|---|---|---|---|
| 1.67 | 0.27 | 1.86 | 0.2 | 0.87 | 0.249 | 0.1173 |

where $m_i = \nu_i\rho_{i0}/\rho_{s0}$ are the mass concentrations of steel ($i = 1$) and concrete ($i = 2$) in the reinforced-concrete layer ($m_1 + m_2 = 1$).

Using the shock-wave relations for the mixture

$$D = v_{s0}\sqrt{p/(v_{s0} - v(p))}, \qquad u = \sqrt{p(v_{s0} - v(p))},$$

we can construct a relation between the shock-wave velocity and the mass velocity and determine the coefficients $c_0$ and $q$.

The velocity of sound $c_0$ is calculated by the formula

$$\frac{1}{c_0} = \sum_{i=1}^{2} \frac{v_i}{c_{i0}}.$$

The Grüneisen coefficient $\gamma_s$ for the mixture is expressed in terms of the Grüneisen coefficients of the components $\gamma_{i0}$:

$$\frac{v_{s0}}{\gamma_s} = \sum_{i=1}^{2} \frac{m_i v_{0i}}{\gamma_{i0}}.$$

The shear modulus $\mu$ and the yield stress $\sigma_T$ of the mixture are given by

$$\mu = 1/(v_1/\mu_{01} + v_2/\mu_{02}), \qquad \sigma_T = m_1\sigma_{s1} + m_2\sigma_{s2},$$

where $\mu_{0i}$ and $\sigma_{si}$ ($i = 1, 2$) are the shear moduli and the yield stresses of the components of the mixture, respectively. In contrast to concrete, which experiences brittle failure, the homogeneous two-phase mixture of steel and concrete fails like a ductile material. As was mentioned above, the limiting value of the relative volume of voids $\xi_*$ is used as the local criterion of cleavage failure in this approach. The local criterion of shear failure is the criterion based on the limiting value of the plastic-deformation work $A_{p*}$. It is assumed that the element of the material fails if $A_p = A_{p*}$. Cracks appear in the element and grow under the action of tensile stresses. The failed material behaves like a granular medium that sustains compressive and shear stresses but has no tensile strength [3, 4, 11].

Provided that

$$p > \frac{y_0}{\alpha k}\Big[\Big(\frac{\alpha}{\alpha - 1}\Big)^{2k/(3-2k)} - 1\Big],$$

the compression of a granular medium is described by the equation

$$\frac{c_{m0}^2\rho_{m0}(1 - 0.5\gamma_{m0}\eta)\eta}{(1 - q_{m0}\eta)^2} + \gamma_{m0}\rho_{m0}\varepsilon - \frac{y_0}{k}\Big[\Big(\frac{\alpha}{\alpha - 1}\Big)^{2k/(3-2k)} - 1\Big] = 0.$$

Under unloading, a granular material cannot sustain tensile stresses; hence, the porosity increases with $p = 0$. The porosity of the material is determined from the equation

$$c_{m0}^2(1 - 0.5\gamma_{m0}\eta)\eta/(1 - q_{m0}\eta)^2 + \gamma_{m0}\varepsilon = 0.$$

The coefficients of adhesion $y_0$ and internal friction $k$ are determined by comparing theoretical and experimental shock adiabats [11].

The behavior of the solid high explosive (HE) under an impact is described by the model of an elastoplastic solid with the use of the hydrodynamic equation of state of the form (1.2). It is assumed that detonation occurs instantaneously in the entire volume. To calculate the expansion of the explosion products of solid high explosives, we use the empirical equation of state [12]

$$p = A\rho^n + \gamma\rho\varepsilon,$$

where $\gamma = \gamma_0 + c\rho$, $c = (\gamma_H - \gamma_0)/\rho_H$, and $\rho_H$ is the density of the explosion products at the Chapman–Jouguet point. The numerical values of the parameters of the equation of state of a 50/50 TNT/RDX HE and its explosion products are listed in Table 1.

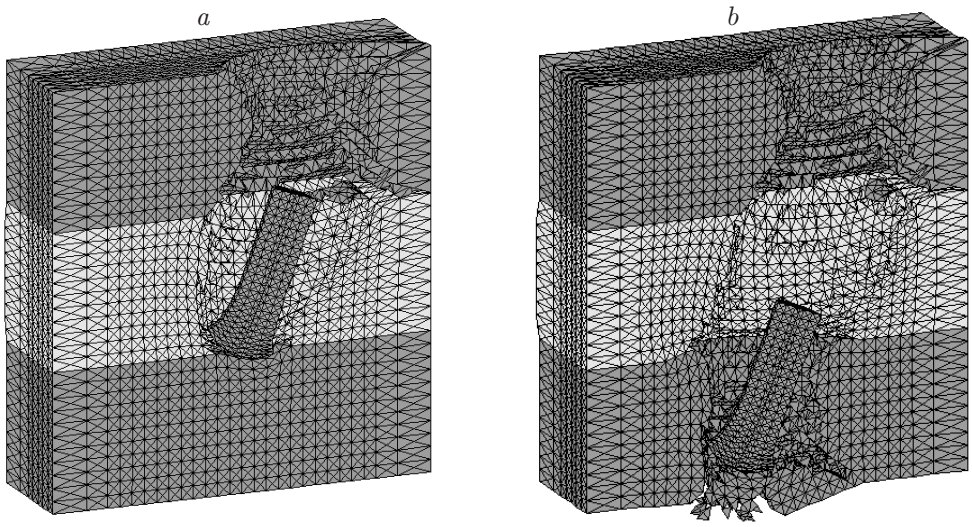


Fig. 2. Layered target hit by a cylindrical steel impactor with a velocity of 800 m/sec and an impact angle of 20° for $t = 92$ (a) and 198 $\mu$sec (b).

**2. Calculation Results.** Using the model proposed above and the numerical method of [13], we solved the problem of penetration of a cylindrical steel impactor with a diameter $d_0 = 7.6$ mm and elongation $4d_0$ into a target consisting of two layers of fine-grain concrete separated by a layer of dry sand. The thickness of each layer was $2.98d_0$. The initial velocity of the impactor was 800 m/sec and the impact angle was 20°. Figure 2 shows the cross sections of isometrical projections of the impactor and target configurations at the times of 92 and 198 $\mu$sec.

An analysis of the calculation results shows that the impactor penetrates through the first concrete layer by the time of 48 $\mu$sec. At this moment, the impactor velocity is 512 m/sec. The impactor passes through the sand layer at 92 $\mu$sec. At this moment, its velocity is 425 m/sec. Subsequent penetration of the impactor into the third layer of concrete is accompanied by its pronounced failure. By the time of 118 $\mu$sec, fragmentation of concrete at the rear surface of the target and separation of the first fragments are observed. At 198 $\mu$sec, along with fine fragments, a large piece of concrete separates from the target and moves downward. When the impactor leaves the rear surface of the target, its velocity is 235 m/sec.

The results of a numerical analysis of interaction of an impactor of similar geometry containing an HE charge and the above-mentioned target under the same impact conditions are described below. Figure 3 shows the cross sections of isometrical projections of the impactor and target at the times of 168 and 170 $\mu$sec. The dark region in the impactor indicates the domain occupied by the HE. An analysis of numerical results shows that the first layer of concrete is punched by 50 $\mu$sec. At this moment, the impactor velocity is 459 m/sec. By 104 $\mu$sec, the impactor passes the sand layer, and its velocity decreases to 363 m/sec.

Since the impactor is actually a steel shell filled by an HE, the deformation of its head part is more pronounced, as compared to the previous case. In addition, the impactor is bent, which was not observed in the previous calculation case.

HE detonation occurs at the moment of 168 $\mu$sec, when the impactor velocity is 191 m/sec. The maximum pressure of HE detonation products is 26 GPa.

At the time of 170 $\mu$sec, the HE decomposition products expand and the steel shell of the impactor is bulged. After that, the fragments of the failed shell interact with the products of the HE reaction with the target materials (sand and concrete). Figure 4 shows the failure pattern of the layered target at the time of 180 $\mu$sec. The impactor and products of HE decomposition are not shown. One can see a catastrophic failure of the target, which is expected to become even more pronounced with time because the maximum pressure of detonation products reaches approximately 5 GPa by this moment.

To study the effect of reinforcement of a concrete slab, we compare the failure patterns of a slab with reinforced layers and a monolithic slab hit by a steel impactor with a velocity of 300 m/sec. The impactor is a

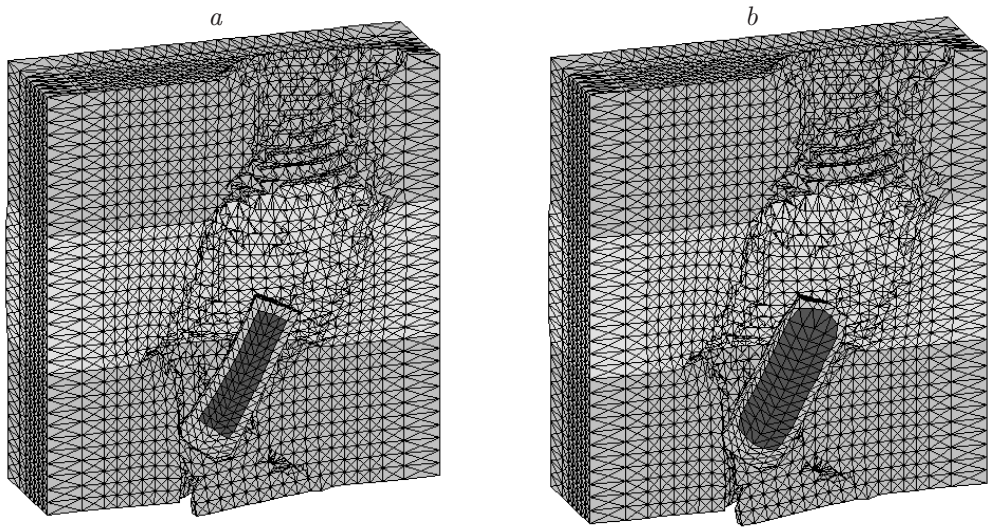


Fig. 3. Penetration of a model projectile into a layered target at a velocity of 800 m/sec and an impact angle of 20° for $t = 168$ (a) and 170 $\mu$sec (b).

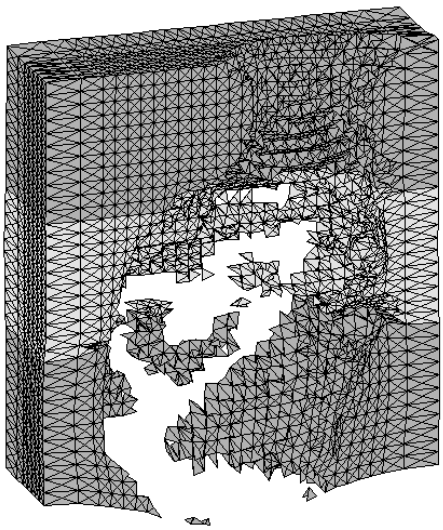

Fig. 4. Failure pattern of a layered target at the moment the numerical calculation is completed.

steel cylinder whose height $h$ is equal to its diameter $d_0$ ($h = d_0 = 300$ mm). The height of the concrete and reinforced-concrete slabs is $H_0 = 2d_0$.

The slab is reinforced by two A-III class reinforcement grids with a cell size of $120 \times 120$ mm and bars 32 mm in diameter. The grids are symmetrical about the mid-surface of the slab with a 30 mm protective layer. Figure 5 shows the failure patterns of concrete and reinforced-concrete slabs obtained at the moment the calculations were completed. The velocities and penetration depths $H/d_0$ of the impactor in the reinforced-concrete and concrete slabs are compared in Table 2 at different times. By 1.8 msec, the impactor in the reinforced-concrete slab passes through the first reinforced layer and penetrates into concrete at a depth $H = 1.16d_0$. At this moment, the penetration velocity of the impactor is 141 m/sec. The slab is subjected to compressive stresses (0.05 GPa $< p <$ 0.19 GPa). As a result of cleavage failure, concrete spalling occurs at the rear surface of the target. By this moment, cleavage failure also begins in the concrete slab, where compressive stresses are almost 1.5 times higher than those in reinforced

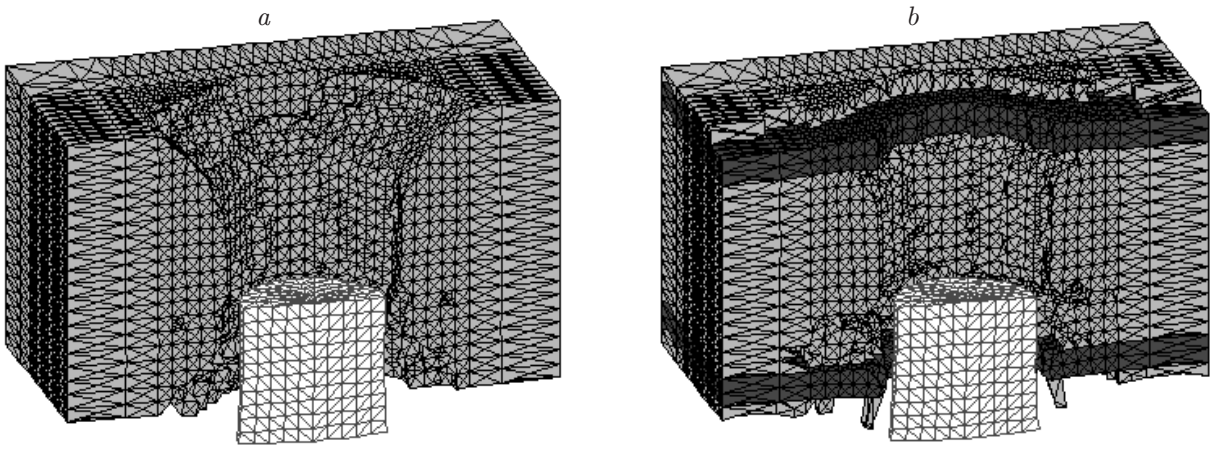


Fig. 5. Failure pattern of a concrete slab (a) and a concrete slab reinforced by a steel grid (b) under a 300 m/sec impact.

TABLE 2

| Time of the process $t$, msec | Reinforced-concrete slab | | Time of the process $t$, msec | Concrete slab | |
|---|---|---|---|---|---|
| | $H/d_0$ | $u$, m/sec | | $H/d_0$ | $u$, m/sec |
| 0.2 | 0.17 | 246 | 0.2 | 0,17 | 254 |
| 0.5 | 0.39 | 214 | 0.5 | 0.42 | 240 |
| 1.8 | 1.16 | 141 | 1.8 | 1.25 | 151 |
| 3.5 | 1.84 | 89 | 3.5 | 1.98 | 119 |
| 4.5 | 2.14 | 85 | 4.3 | 2.3 | 116 |
| 5.2 | 2.34 | 84 | — | — | — |

concrete (0.1 GPa $< p <$ 0.26 GPa). The maximum stresses are reached in the zone where the impactor contacts the target. The relative depth and velocity of penetration into the concrete slab are $H/d_0 = 1.25$ and $u = 151$ m/sec, respectively. The concrete-slab penetration is practically finalized by 3.5 msec. The calculations were completed at 4.3 msec. At the moment the concrete slab is punched, a crater shaped like a structure of two truncated cones with the common base $1.9d_0$ (Fig. 5a) is formed in the slab. The diameters of the upper and lower bases are $2.2d_0$ and $2.1d_0$, respectively. Beyond the target, the impactor velocity is 116 m/sec.

By 3.5 msec, the impactor reaches the second reinforced layer in the reinforced-concrete slab. The penetration velocity decreases to 89 m/sec. Penetration through the second reinforced layer and, hence, the target is completed by 4.5 msec. The calculations were performed until 5.2 msec. Figure 5b shows the pattern of deformation and failure of the reinforced-concrete slab. The reinforced layers of concrete are represented as dark regions.

Beyond the target, the impactor velocity is 85 m/sec. As a result of cleavage failure of the reinforced-concrete slab, complete concrete spalling occurs above the first reinforced layer. Through holes of diameter $1.2d_0$ are formed in both the first and second reinforced layers. Concrete spalling of diameter $3d_0$ occurs on the rear side. The hole in the concrete resembles a figure consisting of a cylinder of diameter $1.2d_0$ and height $0.9d_0$ and a truncated cone whose upper base is the lower base of the cylinder. The lower-base diameter of the truncated cone is $2.2d_0$.

In summary, an analysis of the interactions considered above shows that reinforcement of a concrete slab leads to a 26.7-% decrease in the impactor velocity beyond the target.

This work was supported by the Russian Foundation for Basic Research (Grant No. 04-01-00856).

## REFERENCES


1. N. N. Belov, N. T. Yugov, S. A. Afanas'eva, et al., "Investigation of deformation and failure of brittle materials," *Mekh. Kompoz. Mat. Konstr.*, **7**, No. 2, 131–142 (2001).
2. N. N. Belov, N. T. Yugov, D. G. Kopanitsa, et al., "Computer simulation of dynamic failure in fine-grained concrete," *Vestn. Tomsk. Gos. Arkh. Stroit. Univ.*, No. 1, 14–19 (2001).
3. S. A. Afanas'eva, N. N. Belov, and N. T. Yugov, "Penetration of cylindrical impactors into targets from concrete and sandy soil," *Dokl. Ross. Akad. Nauk*, **387**, No. 5, 1–4 (2002).
4. N. N. Belov, N. T. Yugov, S. A. Afanas'eva, et al., "Penetration of steel impactors into structures from concrete and sandy soil," *Vestn. Tomsk. Gos. Arkh. Stroit. Univ.*, No. 1, 5–12 (2003).
5. V. M. Fomin, A. I. Gulidov, G. A. Sapozhnikov, et al., *High-Velocity Interaction of Solids* [in Russian], Izd. Sib. Otd. Ross. Akad. Nauk, Novosibirsk (1999).
6. N. N. Belov, V. N. Demidov, L. V. Efremova, et al., "Computer simulation of the dynamics of a high-velocity impact and associated physical phenomena," *Izv. Vyssh. Uchebn. Zaved. Fiz.*, **35**, No. 8, 5–48 (1992).
7. R. Kinslow (ed.), *High-Velocity Impact Phenomena*, Academic Press, New York (1970).
8. J. Zykas, T. Nicholas, H. F. Swift, et al., *Impact Dynamics*, John Wiley, New York (1982).
9. A. L. Isaev, "Effect of concrete reinforcement on the results of dynamic loading by penetrating bodies," in: III *Khariton Scientific Readings*, Proc. Int. Conf., Sarov (2020), pp. 150–156.
10. G. A. Geniev and V. N. Kisyuk, "On generalization of the theory of concrete strength," *Beton Zhelezobeton*, No. 2, 16–29 (1965).
11. N. N. Belov, N. T. Yugov, S. A. Afanas'eva, and A. A. Yugov, "Mathematical simulation of penetration of steel impactors into a granular loose medium," *Mekh. Kompoz. Mat. Konstr.*, **10**, No. 1, 108–117 (2004).
12. F. A. Baum, L. P. Orlenko, K. P. Stanyukevich, et al., *Physics of Explosion* [in Russian], Nauka, Moscow (1975).
13. N. T. Yugov, "Numerical analysis of the three-dimensional process of deformation and failure of a cylinder and a plate in an oblique collision," *Izv. Akad. Nauk SSSR, Mekh. Tverd. Tela*, No. 1, 112–117 (1990).